Top-to-bottom Ekman layer and its implications for shallow rotating flows

Cushman-Roisin, Benoit ; Deleersnijder, Eric

DOI
10.1007/s10652-018-9611-y

Publication date
2018

Document Version
Accepted author manuscript

Published in
Environmental Fluid Mechanics

Citation (APA)
Cushman-Roisin, B., & Deleersnijder, E. (2018). Top-to-bottom Ekman layer and its implications for shallow rotating flows. *Environmental Fluid Mechanics*, *19 (2019)*, 1105–1119. https://doi.org/10.1007/s10652-018-9611-y

Top-to-Bottom Ekman Layer and its Implications for Shallow Rotating Flows

Benoit Cushman-Roisin

Thayer School of Engineering
Dartmouth College
Hanover, New Hampshire 03755, USA

Eric Deleersnijder

Institute of Mechanics, Materials and Civil Engineering (IMMC)
& Earth and Life Institute (ELI)
Université catholique de Louvain
4 avenue Georges Lemaître
B-1348 Louvain-la-Neuve, Belgium

Delft Institute of Applied Mathematics (DIAM)
Delft University of Technology
Van Mourik Broekmanweg 6
2628XE Delft, The Netherlands

June 15, 2018

Submitted to *Environmental Fluid Mechanics*
(*Special Shallow Flows Issue*)

ABSTRACT

The analytical solution is derived for rotational frictional flow in a shallow layer of fluid in which the top and bottom Ekman layers join without leaving a frictionless interior. This vertical structure has significant implications for the horizontal flow. In particular, for a layer of water subjected to both a surface wind stress and bottom friction, the vorticity of the horizontal flow is a function not only of the curl of the wind stress (the classical result for deep water known as Ekman pumping) but also of its divergence. The importance of this divergence term peaks for a water depth around 3 times the Ekman layer thickness. This means that a curl-free but non-uniform wind stress on a shallow sea or lake can, through the dual action of rotation and friction, generate vorticity in the wind-driven currents.

We also find that the reduction of three-dimensional dynamics to a two-dimensional model is more subtle than one could have anticipated and needs to be approached with utmost care. Taking the bottom stress as dependent solely on the depth-averaged flow, even with some veering, is not appropriate. The bottom stress ought to include a component proportional to the surface stress, which is negligible for large depths but increases with decreasing water depth.

1 Introduction

The effect of friction in rotating flows is governed by the Ekman number, and it is well known (Price *et al.*, 1987; Cushman-Roisin & Beckers, 2011) that, for an Ekman number much smaller than unity, the role of friction is significant only in thin layers near the top and bottom boundaries, called Ekman layers, and occasionally near lateral boundaries, in so-called Stewartson layers (Bennetts & Hocking, 1973). Away from these boundary layers, in the body of the domain called the *interior*, the effect of friction is felt indirectly. The primary signature is the Ekman pumping, a vertical velocity that starts at the base of the top Ekman layer as proportional to the curl of the surface stress and ends at the top of the bottom Ekman layer as proportional to the curl of the bottom stress. On the $\beta-$plane, the surface and bottom stresses may differ, and the Ekman velocity may vary over the vertical, but on an $f-$plane, the Ekman pumping velocity must be uniform over the vertical, and the surface and bottom stresses be equal (Cushman-Roisin & Beckers, 2011).

The situation becomes much more complex when the rotating domain is shallow enough for the top and bottom Ekman layers to merge, leaving no frictionless interior. The behavior of the vertical velocity is much richer, and the concept of Ekman pumping is no longer helpful. The bibliography of this work is limited because, although the governing equations are straightforward, the analytical solution of the linearized problem is tedious and tends to obscure the properties of the flow.

Extending Ekman's second paper on frictional rotating flows (Ekman, 1923) and with the focus on storm surges in shallow seas, Welander (1957) considered the case when "the depth of frictional influence" is comparable to the water depth and arrived at the conclusion that the wind-stress divergence may be of the same importance as the wind-stress curl in governing the streamfunction of the depth-averaged flow, but he did not consider the vertical velocity and quickly proceeded to the time-dependent case of a storm surge. In the 1970s, when electronic computers first became available and used for storm surge forecasting, they were not yet capable of handling three-dimensional grids, and a flurry of work ensued to reduce the 3D equations to 2D equations by pre-solving for the vertical profile of the horizontal velocity. This work (Jelesnianski, 1970; Forristall, 1974; Cheng *et al.*, 1976; Nihoul, 1977) largely focused on the effects of a vertically varying eddy viscosity to obtain the bottom stress in terms of the depth-averaged horizontal velocity. No attention was paid to the vertical velocity. A decade later, as 3D numerical models came into being, Lynch and Officer (1985) paid renewed attention to the vertical structure of viscous rotating flow in order to provide analytic solutions as test cases for 3D hydrodynamic models. Like their predecessors, they chose depth-varying eddy viscosities and took the bottom stress as aligned with and proportional to the depth-averaged velocity. Their solutions are cast as solutions to an eigenvalue problem in the vertical, which requires the numerical solution of a 1D equation.

In this work, we ask different questions: What happens to the concept of Ekman pumping when the Ekman number is not small? What is the vertical profile of the vertical velocity? How do local wind-stress curl and divergence affect the depth-averaged flow? And, under which conditions can the bottom stress be taken as parallel to the depth-averaged velocity? The answer to the latter points to unexpected difficulties in the reduction of 3D dynamics to a 2D model and might cast doubts on the accuracy of past 2D models.

2 Top-to-Bottom Ekman Dynamics

We are considering a shallow flow of water of uniform density subject to an imposed surface stress at the top and no slip along a flat horizontal bottom.

We solve the classical Ekman dynamics problem in the context of the following assumptions: f-plane (with $f > 0$ for convenience), low-Rossby number (to permit the neglect of nonlinear advection terms and facilitate the analysis), hydrostatic balance ($\partial p/\partial z = -\rho g$), constant density ρ (no stratification), flat bottom and rigid lid ($-H \le z \le 0$, $H =$ constant), eddy viscosity model with uniform eddy viscosity ν,

and imposed surface wind stress (τ_x, τ_y functions of x and y).

We recognize that the neglect of the temporal derivatives and nonlinear advection terms is not justified in many circumstances, but we nonetheless ignore those terms here to place the focus on the combined role of Coriolis and friction forces in a mathematically tractable fashion, with the underlying hypothesis that the main findings of our study will continue to hold at least qualitatively in the broader dynamical setting that includes temporal derivatives and nonlinear advection terms. It also happens that the assumption of a low Rossby number and temporal Rossby number is justifiable whenever the scales of the problem obey the following relations:

$$Ek = \frac{\nu}{fH^2} \geq 1, \qquad Ro = \frac{U}{fL} = \frac{\tau}{\rho f^2 HL} \ll 1, \qquad Ro_T = \frac{1}{fT} \ll 1, \tag{1}$$

in which L and U are horizontal length and velocity scales, T is the time scale, and τ is a scale for the wind stress. Such relations are not unrealistic for shallow water flows. For example, the values $f \sim 10^{-4}$/s, $H \sim 10$ m, $L \sim 10$ km, $T \sim 2 \times 10^5$ s (= several days), $\tau/\rho \sim 10^{-4}$ m^2/s^2, friction velocity $u_* = \sqrt{\tau/\rho} \sim 10^{-2}$ m/s, $U \sim \tau/\rho f H \sim 0.1$ m/s, and $\nu \sim u_* H \sim 10^{-1}$ m^2/s do meet the preceding criteria ($Ek \sim 10$, $Ro \sim 0.1$, and $Ro_T \sim 0.05$).

We begin the analysis by expressing the horizontal pressure gradient force in terms of geostrophic flow components:

$$-f v_g = -\frac{1}{\rho}\frac{\partial p}{\partial x} \tag{2}$$

$$+f u_g = -\frac{1}{\rho}\frac{\partial p}{\partial y}\,, \tag{3}$$

from which follows that on an f-plane, the geostrophic flow is without divergence:

$$\frac{\partial u_g}{\partial x} + \frac{\partial v_g}{\partial y} = 0. \tag{4}$$

It is also z-independent by virtue of the hydrostatic balance with constant density.

The equations governing the three velocity components u, v and w are:

$$-f v = -f v_g + \nu \frac{\partial^2 u}{\partial z^2} \tag{5}$$

$$+f u = +f u_g + \nu \frac{\partial^2 v}{\partial z^2} \tag{6}$$

$$\frac{\partial u}{\partial x} + \frac{\partial v}{\partial y} + \frac{\partial w}{\partial z} = 0. \tag{7}$$

There are three boundary conditions at each horizontal boundary.

- At the bottom, we impose no flow on the frictional and impermeable bottom:

$$u = v = w = 0 \quad \text{at} \quad z = -H. \tag{8}$$

- At the top, we impose a surface wind stress and no vertical flow through the rigid lid:

$$\rho\nu \frac{\partial u}{\partial z} = \tau_x, \quad \rho\nu \frac{\partial v}{\partial z} = \tau_y, \quad w = 0 \quad \text{at} \quad z = 0. \tag{9}$$

The rigid-lid approximation ($w = 0$) is made for the same reason as stated above, namely to keep the focus on the combined role of Coriolis and friction forces with a minimum of other dynamics.

We note that the set of Equations (5)-(6)-(7) contains a total of five z-derivatives while we have specified six boundary conditions in the z-direction. Thus, the system is over-specified by one, and we ought to expect a constraint on some of the variables that enter the equations, particularly a relationship between the geostrophic velocity (u_g, v_g), which is the horizontal pressure gradient in disguise, and the wind stress (τ_x, τ_y).

The situation can be anticipated by considering the case of a deep water column compared to the Ekman layer thickness, defined as

$$d = \sqrt{\frac{2\nu}{f}} \ . \tag{10}$$

If $d \ll H$, friction is significant only in top and bottom boundary layers that occupy much less than the water depth, leaving a frictionless and geostrophic interior. In this case, surface Ekman dynamics generates a so-called Ekman pumping vertical velocity through the interior (Cushman-Roisin and Beckers, page 254) proportional to the wind stress curl:

$$w_{interior} = \frac{1}{\rho f} \ \left(\frac{\partial \tau_y}{\partial x} - \frac{\partial \tau_x}{\partial y} \right) \ , \tag{11}$$

while bottom Ekman dynamics generate an interior vertical velocity proportional to the vorticity of the geostrophic flow (Cushman-Roisin and Beckers, page 249):

$$w_{interior} = \frac{d}{2} \ \left(\frac{\partial v_g}{\partial x} - \frac{\partial u_g}{\partial y} \right) \ . \tag{12}$$

Given that the vertical velocity in the interior takes a unique value because the interior geostrophic flow has no divergence, it follows that the preceding expressions must be equal to each other:

$$\frac{\partial v_g}{\partial x} - \frac{\partial u_g}{\partial y} = \frac{2}{\rho f d} \ \left(\frac{\partial \tau_y}{\partial x} - \frac{\partial \tau_x}{\partial y} \right) \ . \tag{13}$$

In other words, in water deep compared to the Ekman layer thickness, the vorticity of the interior geostrophic flow is constrained to be proportional to the curl of the surface wind stress, a local dependency. The primary aim of this study is to determine how this relationship is affected when the water depth is comparable to the Ekman layer thickness ($d \sim H$, i.e. $\nu / f H^2 \sim 1$) and friction affects the entire water column.

At this point, we could proceed to solve Equations (5)-(6) for u and v, but the algebra is very tedious (Welander, 1957). A more efficient path toward the relationship we seek is not to solve for the velocity components themselves but for their divergence $\partial u/\partial x + \partial v/\partial y$ and vorticity $\partial v/\partial x - \partial u/\partial y$. For this, we differentiate Equations (5)-(6) and combine to obtain the following coupled equations for the divergence and vorticity:

$$f \ \left(\frac{\partial u}{\partial x} + \frac{\partial v}{\partial y} \right) \ = \ f \ \left(\frac{\partial u_g}{\partial x} + \frac{\partial v_g}{\partial y} \right) + \nu \frac{\partial^2}{\partial z^2} \left(\frac{\partial v}{\partial x} - \frac{\partial u}{\partial y} \right) \tag{14}$$

$$f \ \left(\frac{\partial v}{\partial x} - \frac{\partial u}{\partial y} \right) \ = \ f \ \left(\frac{\partial v_g}{\partial x} - \frac{\partial u_g}{\partial y} \right) - \nu \frac{\partial^2}{\partial z^2} \left(\frac{\partial u}{\partial x} + \frac{\partial v}{\partial y} \right) \ . \tag{15}$$

In (14), the divergence of the geostrophic flow vanishes by virtue of (4), and the general solution of the equations can be written as:

$$\frac{\partial u}{\partial x} + \frac{\partial v}{\partial y} \ = \ \cosh \zeta \ (D \cos \zeta - C \sin \zeta) + \sinh \zeta \ (B \cos \zeta - A \sin \zeta) \tag{16}$$

$$\frac{\partial v}{\partial x} - \frac{\partial u}{\partial y} \ = \ \frac{\partial v_g}{\partial x} - \frac{\partial u_g}{\partial y} + \cosh \zeta \ (A \cos \zeta + B \sin \zeta) + \sinh \zeta \ (C \cos \zeta + D \sin \zeta) \tag{17}$$

in which the dimensionless vertical coordinate ζ is defined by

$$\zeta = \frac{z+H}{d} \ . \tag{18}$$

It vanishes at the bottom and reaches H/d at the surface.

The four constants of integration A, B, C and D are determined by the application of top and bottom boundary conditions. The horizontal velocity vanishes along the bottom ($\zeta = 0$), and so must its divergence and vorticity. This determines the coefficients A and D:

$$A = -\left(\frac{\partial v_g}{\partial x} - \frac{\partial u_g}{\partial y}\right) \ , \qquad D = 0. \tag{19}$$

Before applying boundary conditions at the surface, it is necessary to determine the vertical velocity across the water column, which is obtained by integrating the continuity equation vertically, starting from $w = 0$ at the bottom:

$$\begin{aligned} w &= -\int_0^z \left(\frac{\partial u}{\partial x} + \frac{\partial v}{\partial y}\right) \, dz' \\ &= -d\int_0^\zeta \left[-C\cosh\zeta' \ \sin\zeta' + \sinh\zeta' \ (B\cos\zeta' - A\sin\zeta')\right] \, d\zeta' \\ &= \frac{d}{2}(B+C)(1-\cosh\zeta\cos\zeta) - \frac{d}{2}(B-C)\sinh\zeta\sin\zeta \\ &+ \frac{d}{2}A \ (\cosh\zeta\sin\zeta - \sinh\zeta\cos\zeta). \end{aligned} \tag{20}$$

Enforcing $w = 0$ at the surface ($z = 0$, $\zeta = H/d$) yields:

$$A \ \left(\cosh\frac{H}{d}\sin\frac{H}{d} - \sinh\frac{H}{d}\cos\frac{H}{d}\right) + (B+C)\left(1 - \cosh\frac{H}{d}\cos\frac{H}{d}\right) - (B-C)\sinh\frac{H}{d}\sin\frac{H}{d} = 0 \ . \tag{21}$$

The application of the remaining two boundary conditions at the surface, which involve the surface wind stress, necessitates the preliminary taking of the z-derivative of the divergence and vorticity:

$$\begin{aligned} \frac{\partial}{\partial z}\left(\frac{\partial u}{\partial x} + \frac{\partial v}{\partial y}\right) &= \frac{1}{d} \ [(B-C)\cosh\zeta\cos\zeta - (B+C)\sinh\zeta\sin\zeta] \\ &- \frac{1}{d} \ A(\cosh\zeta\sin\zeta + \sinh\zeta\cos\zeta) \end{aligned} \tag{22}$$

$$\begin{aligned} \frac{\partial}{\partial z}\left(\frac{\partial v}{\partial x} - \frac{\partial u}{\partial y}\right) &= \frac{1}{d} \ [(B+C)\cosh\zeta\cos\zeta + (B-C)\sinh\zeta\sin\zeta] \\ &- \frac{1}{d} \ A(\cosh\zeta\sin\zeta - \sinh\zeta\cos\zeta) \ . \end{aligned} \tag{23}$$

The stress boundary conditions (9) can now be applied at the top ($\zeta = H/d$):

$$\begin{aligned} \frac{\partial\tau_x}{\partial x} + \frac{\partial\tau_y}{\partial y} &= \frac{\rho f d}{2} \ \left[(B-C)\cosh\frac{H}{d}\cos\frac{H}{d} - (B+C)\sinh\frac{H}{d}\sin\frac{H}{d}\right] \\ &- \frac{\rho f d}{2} \ A\left(\cosh\frac{H}{d}\sin\frac{H}{d} + \sinh\frac{H}{d}\cos\frac{H}{d}\right) \end{aligned} \tag{24}$$

$$\begin{aligned} \frac{\partial\tau_y}{\partial x} - \frac{\partial\tau_x}{\partial y} &= \frac{\rho f d}{2} \ \left[(B+C)\cosh\frac{H}{d}\cos\frac{H}{d} + (B-C)\sinh\frac{H}{d}\sin\frac{H}{d}\right] \\ &- \frac{\rho f d}{2} \ A\left(\cosh\frac{H}{d}\sin\frac{H}{d} - \sinh\frac{H}{d}\cos\frac{H}{d}\right) \ . \end{aligned} \tag{25}$$

Since the coefficient A is already known in terms of the vorticity of the geostrophic flow [see (19)], the preceding two equations form a 2×2 system of equations for $B-C$ and $B+C$. The solution is:

$$\begin{aligned} B-C = &\frac{2}{\rho f d\Delta}\left(\frac{\partial\tau_y}{\partial x}-\frac{\partial\tau_x}{\partial y}\right)\sinh\frac{H}{d}\sin\frac{H}{d} \\ &+\frac{2}{\rho f d\Delta}\left(\frac{\partial\tau_x}{\partial x}+\frac{\partial\tau_y}{\partial y}\right)\cosh\frac{H}{d}\cos\frac{H}{d} \\ &-\frac{1}{\Delta}\left(\frac{\partial v_g}{\partial x}-\frac{\partial u_g}{\partial y}\right)\left(\cosh\frac{H}{d}\sinh\frac{H}{d}+\cos\frac{H}{d}\sin\frac{H}{d}\right) \end{aligned} \tag{26}$$

$$\begin{aligned} B+C = &\frac{2}{\rho f d\Delta}\left(\frac{\partial\tau_y}{\partial x}-\frac{\partial\tau_x}{\partial y}\right)\cosh\frac{H}{d}\cos\frac{H}{d} \\ &-\frac{2}{\rho f d\Delta}\left(\frac{\partial\tau_x}{\partial x}+\frac{\partial\tau_y}{\partial y}\right)\sinh\frac{H}{d}\sin\frac{H}{d} \\ &+\frac{1}{\Delta}\left(\frac{\partial v_g}{\partial x}-\frac{\partial u_g}{\partial y}\right)\left(\cosh\frac{H}{d}\sinh\frac{H}{d}-\cos\frac{H}{d}\sin\frac{H}{d}\right)\ , \end{aligned} \tag{27}$$

after A was replaced by its value given in (19) and with Δ, the determinant of the system, defined as

$$\begin{aligned} \Delta &= \cosh^2\frac{H}{d}\cos^2\frac{H}{d}+\sinh^2\frac{H}{d}\sin^2\frac{H}{d} \\ &= \sinh^2\frac{H}{d}+\cos^2\frac{H}{d}. \end{aligned} \tag{28}$$

Substitution in (21) yields the sought-after relationship between the geostrophic flow and the wind stress:

$$\begin{aligned} &\left(\frac{\partial v_g}{\partial x}-\frac{\partial u_g}{\partial y}\right)\left(\cosh\frac{H}{d}\sinh\frac{H}{d}-\cos\frac{H}{d}\sin\frac{H}{d}\right) \\ &=\frac{2}{\rho f d}\left(\frac{\partial\tau_y}{\partial x}-\frac{\partial\tau_x}{\partial y}\right)\left(\cosh^2\frac{H}{d}+\cos^2\frac{H}{d}-\cosh\frac{H}{d}\cos\frac{H}{d}-1\right) \\ &+\frac{2}{\rho f d}\left(\frac{\partial\tau_x}{\partial x}+\frac{\partial\tau_y}{\partial y}\right)\sinh\frac{H}{d}\sin\frac{H}{d}\ . \end{aligned} \tag{29}$$

This last equation is the relation between the geostrophic flow (u_g, v_g), and the wind stress (τ_x, τ_y) that extends Equation (13) to the case of shallow water ($d\sim H$, i.e. $\nu/fH^2\sim 1$). It was derived by Welander (1957, Equation (17)) albeit as a more complicated mathematical expression. We note that the vorticity of the geostrophic flow is no longer simply proportional to the curl of the wind stress but is now a linear combination of both curl and divergence of the wind stress. In the limit $H\gg d$, Equation (29) reverts to (13) as it should.

To better discern the dependency of the geostrophic vorticity on the curl and divergence of the wind stress, we rewrite (29) as:

$$\left(\frac{\partial v_g}{\partial x}-\frac{\partial u_g}{\partial y}\right)=\frac{2}{\rho f d}\,F\left(\frac{H}{d}\right)\,\left(\frac{\partial\tau_y}{\partial x}-\frac{\partial\tau_x}{\partial y}\right)+\frac{2}{\rho f H}\,G\left(\frac{H}{d}\right)\,\left(\frac{\partial\tau_x}{\partial x}+\frac{\partial\tau_y}{\partial y}\right)\ , \tag{30}$$

in which F and G are dimensionless functions of the dimensionless variable H/d. These are plotted on Figure 1. We note that, for $H>7d$, $F\simeq 1$ and $G\simeq 0$, corresponding to the deep-water situation with geostrophic vorticity proportional to the wind-stress curl only. In the limit $H/d=0$, F vanishes, $G=\frac{3}{4}$, and the situation has flipped with the geostrophic vorticity now purely proportional to the wind-stress divergence. Note that in the transition regime ($0<H<7d$), F reaches a maximum of 1.225, which exceeds its asymptotic value 1, and G reaches a minimum of -0.1113, which falls below its asymptotic value of 0.

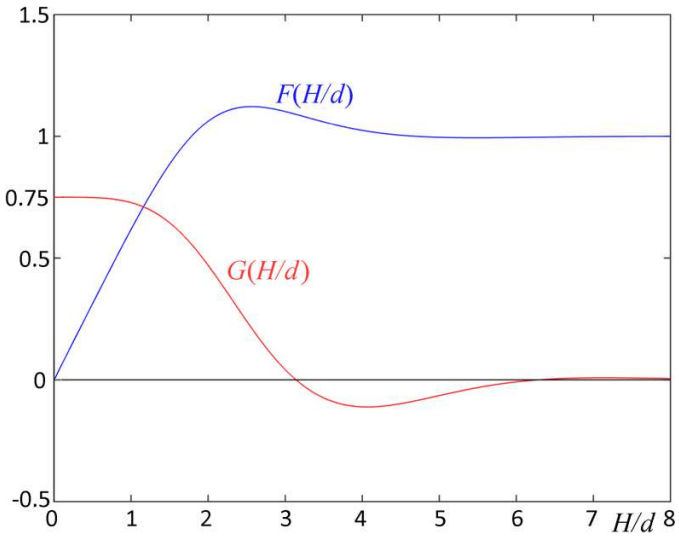

Figure 1: The dimensionless functions F and G of the thickness ratio H/d. The function F provides the dependence of the geostrophic vorticity on the wind-stress curl, and G on the wind-stress divergence.

Caution is in order. When the water column is deep, the interior geostrophic flow is asymptotically equal to the depth-averaged flow, but is no longer so in the case of shallow water because Ekman dynamics act over the entire water column. Thus, we need to make a distinction between the geostrophic component of the flow and the depth-averaged flow.

We define the depth-averaged velocity as

$$\bar{u} = \frac{1}{H}\int_{-H}^{0} u\, dz \quad , \qquad \bar{v} = \frac{1}{H}\int_{-H}^{0} v\, dz \quad . \tag{31}$$

Vertical integration of Equations (14)-(15) from top to bottom† followed by utilization of boundary conditions (9) and use of (22)-(23) provides:

$$\frac{\partial \bar{u}}{\partial x} + \frac{\partial \bar{v}}{\partial y} = \frac{1}{\rho f H}\left(\frac{\partial \tau_y}{\partial x} - \frac{\partial \tau_x}{\partial y}\right) - \frac{d}{2H}(B+C) \tag{32}$$

$$\frac{\partial \bar{v}}{\partial x} - \frac{\partial \bar{u}}{\partial y} = \left(\frac{\partial v_g}{\partial x} - \frac{\partial u_g}{\partial y}\right) - \frac{1}{\rho f H}\left(\frac{\partial \tau_x}{\partial x} + \frac{\partial \tau_y}{\partial y}\right) + \frac{d}{2H}(B-C). \tag{33}$$

Further replacement of $B+C$ and $B-C$ by their values given in (27)-(26) leads to:

$$\begin{aligned}\frac{\partial \bar{u}}{\partial x} + \frac{\partial \bar{v}}{\partial y} = &-\frac{d}{2H\Delta}\left(\frac{\partial v_g}{\partial x} - \frac{\partial u_g}{\partial y}\right)\left(\cosh\frac{H}{d}\sinh\frac{H}{d} - \cos\frac{H}{d}\sin\frac{H}{d}\right)\\ &+ \frac{1}{\rho f H}\left(\frac{\partial \tau_y}{\partial x} - \frac{\partial \tau_x}{\partial y}\right)\left(1 - \frac{1}{\Delta}\cosh\frac{H}{d}\cos\frac{H}{d}\right)\\ &+ \frac{1}{\rho f H}\left(\frac{\partial \tau_x}{\partial x} + \frac{\partial \tau_y}{\partial y}\right)\frac{1}{\Delta}\sinh\frac{H}{d}\sin\frac{H}{d}\end{aligned} \tag{34}$$

$$\begin{aligned}\frac{\partial \bar{v}}{\partial x} - \frac{\partial \bar{u}}{\partial y} = &\left(\frac{\partial v_g}{\partial x} - \frac{\partial u_g}{\partial y}\right)\left[1 - \frac{d}{2H\Delta}\left(\cosh\frac{H}{d}\sinh\frac{H}{d} + \cos\frac{H}{d}\sin\frac{H}{d}\right)\right]\\ &+ \frac{1}{\rho f H}\left(\frac{\partial \tau_y}{\partial x} - \frac{\partial \tau_x}{\partial y}\right)\frac{1}{\Delta}\sinh\frac{H}{d}\sin\frac{H}{d}\\ &- \frac{1}{\rho f H}\left(\frac{\partial \tau_x}{\partial x} + \frac{\partial \tau_y}{\partial y}\right)\left(1 - \frac{1}{\Delta}\cosh\frac{H}{d}\cos\frac{H}{d}\right) \quad .\end{aligned} \tag{35}$$

†Note that this demands a flat horizontal bottom, which we had assumed from the start.

Finally, elimination of the vorticity of the geostrophic flow by use of (29) provides:

$$\frac{\partial \bar{u}}{\partial x} + \frac{\partial \bar{v}}{\partial y} = 0, \tag{36}$$

and

$$\frac{\partial \bar{v}}{\partial x} - \frac{\partial \bar{u}}{\partial y} = \frac{2}{\rho f d}\, \bar{F}\left(\frac{H}{d}\right)\, \left(\frac{\partial \tau_y}{\partial x} - \frac{\partial \tau_x}{\partial y}\right) - \frac{2}{\rho f d}\, \bar{G}\left(\frac{H}{d}\right)\, \left(\frac{\partial \tau_x}{\partial x} + \frac{\partial \tau_y}{\partial y}\right)\ . \tag{37}$$

The first of these equations returns the expected result that the depth-averaged flow has no divergence (incompressible flow between two parallel impermeable boundaries), while the second equation is the constraint on the flow [Equation (29)] now expressed in terms of the vorticity of the depth-averaged flow. This equation was first derived by Welander (1957, Equation (26)), but no discussion was provided other than pointing out that there is a dependency on the wind-stress divergence.

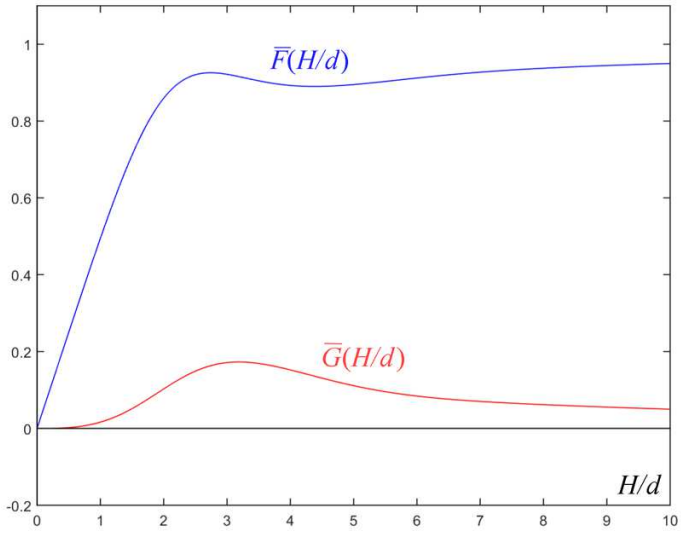

Figure 2: The dimensionless functions $\bar{F}$ and $\bar{G}$ of the thickness ratio H/d. The function $\bar{F}$ provides the dependence of the depth-averaged vorticity on the wind-stress curl, and $\bar{G}$ on the wind-stress divergence.

Figure 2 shows the dependency of the $\bar{F}$ and $\bar{G}$ functions on the thickness ratio H/d. The dependency of the depth-averaged vorticity on the wind-stress curl ($\bar{F}$ function) is fairly similar to that of the geostrophic vorticity (F function), starting from 0 and asymptoting to 1; the intermediate maximum now is 0.9259, and there is an intermediate minimum of 0.8903. In contrast, the dependency on the wind-stress divergence is quite different. First, there is a reversal in sign (not shown in Figure 2 but made explicit in Equation (37)). In deep water ($H/d \to \infty$), it slowly vanishes; in the shallow limit ($H/d \to 0$), the function $\bar{G}$ reaches zero more rapidly than the function $\bar{F}$, implying that, when $H << d$, the wind-stress curl remains the dominant contribution to the depth-averaged vorticity (as shown in the next section). The function $\bar{G}$ reaches a maximum of 0.1730 for $H/d = 3.17$. In other words, the contribution of the wind-stress divergence to the depth-averaged vorticity is only significant at intermediate depths. Figure 3 displays the ratio of the coefficients of the divergence and curl terms in (37) (without the minus sign). We note that it reaches a maximum of 0.1891 (19%) at $H/d = 3.265$.

3 Case of Very Shallow Flow

Because the coefficients that arise in the preceding expressions are complicated functions of the ratio H/d, it is worthwhile to consider the limit of a very shallow layer (or weakly rotating flow). To do this, we take

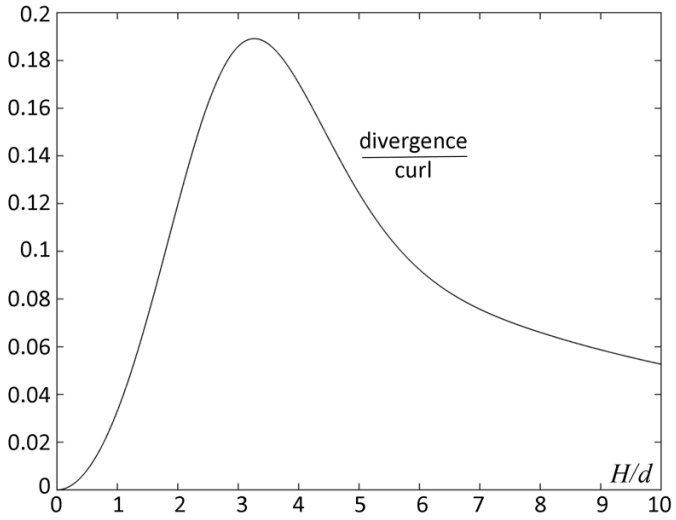

Figure 3: The ratio of the coefficients of the divergence and curl terms in Equation (37).

the limit $H/d \to 0$ in both (29) and (35). At the leading order, these equations become, respectively:

$$\frac{\partial v_g}{\partial x} - \frac{\partial u_g}{\partial y} \simeq \frac{3}{2\rho f H}\left(\frac{\partial \tau_x}{\partial x} + \frac{\partial \tau_y}{\partial y}\right) \tag{38}$$

$$\frac{\partial \bar{v}}{\partial x} - \frac{\partial \bar{u}}{\partial y} \simeq \frac{H}{\rho f d^2}\left(\frac{\partial \tau_y}{\partial x} - \frac{\partial \tau_x}{\partial y}\right) . \tag{39}$$

We note from Equation (38) that the vorticity of the geostrophic flow is now proportional to the divergence of the wind stress, a complete flip from (13) where it was proportional to the curl of the wind stress. Equation (39) for the depth-averaged flow is similar to (13) but with a coefficient that has an extra power of the ratio H/d.

4 Implications for 2D Modeling

Let us suppose that we had not bothered about 3D Ekman dynamics and instead had used the following two-dimensional model with linear friction:

$$-f\bar{v} = -fv_g + \frac{\tau_x}{\rho H} - r\bar{u} \tag{40}$$

$$+f\bar{u} = +fu_g + \frac{\tau_y}{\rho H} - r\bar{v} \tag{41}$$

$$\frac{\partial \bar{u}}{\partial x} + \frac{\partial \bar{v}}{\partial y} = 0, \tag{42}$$

in which the wind stress is applied as a body force and r is a friction coefficient, which should be related to the viscosity ν somehow. We use overbars on the velocity components to indicate that these are vertically uniform, *i.e.* they are depth averages. Thus, this model assumes a bottom stress counter-aligned with the depth-averaged velocity. Such a 2D model, often extended to include time derivatives, nonlinear advection terms, and a quadratic expression for the bottom stress has long been a staple of wind-driven circulation modeling for lakes and coastal areas (Heaps, 1969 - Equation (5); Lick, 1976 - Page 58; Schwab, 1983 - Equation (4); Lentz *et al.*, 1999 - Equation (5); Weisberg & Zhang, 2008 - Equation (8); Józsa, 2014 - Equation (13); to cite only one study per decade).

We ask what value should be given to the friction coefficient r in terms of the kinematic viscosity ν and the other parameters in the formalism, f and H, in such a way as to render this 2D model an exact representation of the 3D model after elimination of the vertical structure of the flow. For this, we begin by solving the momentum equations (40)-(41) for $\bar{u}$ and $\bar{v}$, which is straightforward:

$$\bar{u} = \frac{f^2}{f^2+r^2}\, u_g - \frac{rf}{f^2+r^2}\, v_g + \frac{1}{\rho H(f^2+r^2)}\,(r\tau_x + f\tau_y) \tag{43}$$

$$\bar{v} = \frac{f^2}{f^2+r^2}\, v_g + \frac{rf}{f^2+r^2}\, u_g + \frac{1}{\rho H(f^2+r^2)}\,(r\tau_y - f\tau_x)\ , \tag{44}$$

and then proceed by taking the divergence $\partial\bar{u}/\partial x + \partial\bar{v}/\partial y$, which we set to zero as continuity (42) demands. The result is:

$$\frac{\partial v_g}{\partial x} - \frac{\partial u_g}{\partial y} = \frac{1}{\rho r H}\left(\frac{\partial \tau_y}{\partial x} - \frac{\partial \tau_x}{\partial y}\right) + \frac{1}{\rho f H}\left(\frac{\partial \tau_x}{\partial x} + \frac{\partial \tau_y}{\partial y}\right)\ , \tag{45}$$

which is isomorphic to (30) in that the vorticity of the geostrophic flow is a linear combination of the divergence and curl of the wind stress. Mapping (45) onto (29) demands the following two equivalencies:

$$\frac{r}{f} = \frac{d}{2H}\ \frac{\cosh\frac{H}{d}\sinh\frac{H}{d} - \cos\frac{H}{d}\sin\frac{H}{d}}{\cosh^2\frac{H}{d} + \cos^2\frac{H}{d} - \cosh\frac{H}{d}\cos\frac{H}{d} - 1} \tag{46}$$

$$\frac{2H}{d}\sinh\frac{H}{d}\sin\frac{H}{d} = \cosh\frac{H}{d}\sinh\frac{H}{d} - \cos\frac{H}{d}\sin\frac{H}{d}\ . \tag{47}$$

While the first of these equations serves to set the value for the friction coefficient r in terms of the viscosity ν (subsumed in d), the second equation ought to be satisfied, too. A glance at this equation reveals that it is impossible to satisfy it for an arbitrary value[†] of the ratio H/d. Thus, we are brought to conclude that the reduced two-dimensional model (40)-(41)-(42) is not a legitimate reduction of the three-dimensional model (5)-(6)-(7).

One may think at this point that the veering involved in Ekman dynamics should cause the bottom stress to be at a non-zero angle to the mean velocity and that the presence of this angle would resolve the matter. Surprisingly, however, it does not: Equation (47) arises once again. A non-intuitive remedy is to turn the surface wind stress by a certain angle. This does not seem to have a physical basis until one thinks of it as a parameterization of the bottom stress as a linear combination of the mean velocity and surface stress rather than being dependent on the mean velocity alone.

For an angle α of rotation, positive in the trigonometric sense, we try 2D equations of the form:

$$-f\bar{v} = -fv_g + \frac{\cos\alpha\ \tau_x - \sin\alpha\ \tau_y}{\rho H} - r\bar{u} \tag{48}$$

$$+f\bar{u} = +fu_g + \frac{\sin\alpha\ \tau_x + \cos\alpha\ \tau_y}{\rho H} - r\bar{v} \tag{49}$$

$$\frac{\partial\bar{u}}{\partial x} + \frac{\partial\bar{v}}{\partial y} = 0. \tag{50}$$

of which the solution for $\bar{u}$ and $\bar{v}$ is:

$$\bar{u} = \frac{f^2u_g - rfv_g}{f^2+r^2} + \frac{(f\sin\alpha + r\cos\alpha)\tau_x + (f\cos\alpha - r\sin\alpha)\tau_y}{\rho H(f^2+r^2)} \tag{51}$$

$$\bar{v} = \frac{f^2v_g + rfu_g}{f^2+r^2} + \frac{(f\sin\alpha + r\cos\alpha)\tau_y - (f\cos\alpha - r\sin\alpha)\tau_x}{\rho H(f^2+r^2)}\ , \tag{52}$$

[†]Not even in the asymptotic cases of very small or very large values.

with the following zero-divergence condition:

$$\frac{\partial v_g}{\partial x} - \frac{\partial u_g}{\partial y} = \frac{f\cos\alpha - r\sin\alpha}{\rho r f H}\left(\frac{\partial \tau_y}{\partial x} - \frac{\partial \tau_x}{\partial y}\right) + \frac{f\sin\alpha + r\cos\alpha}{\rho r f H}\left(\frac{\partial \tau_x}{\partial x} + \frac{\partial \tau_y}{\partial y}\right) \ . \tag{53}$$

Mapping (53) onto (29) demands the following two equivalencies:

$$\frac{f}{r}\cos\alpha - \sin\alpha = \frac{2H}{d}\ \frac{\cosh^2\frac{H}{d} + \cos^2\frac{H}{d} - \cosh\frac{H}{d}\cos\frac{H}{d} - 1}{\cosh\frac{H}{d}\sinh\frac{H}{d} - \cos\frac{H}{d}\sin\frac{H}{d}} \tag{54}$$

$$\frac{f}{r}\sin\alpha + \cos\alpha = \frac{2H}{d}\ \frac{\sinh\frac{H}{d}\sin\frac{H}{d}}{\cosh\frac{H}{d}\sinh\frac{H}{d} - \cos\frac{H}{d}\sin\frac{H}{d}} \ . \tag{55}$$

Both conditions can now be met as the two conditions now form a 2×2 system of equations for the two unknowns r/f and α. Figure 4 displays the variations of the ratio r/f (magnified by a factor 100) and angle α as functions of the thickness ratio H/d. As can be expected, both vanish for great depths (with $r/f \simeq d/2H$). As the water depth decreases, friction becomes more important, as expected, and the angle α swings between a minimum of $-8.910°$ and a maximum of $+48.17°$. The angle α becomes appreciable ($|\alpha| > 5°$) when H/d falls below 6.

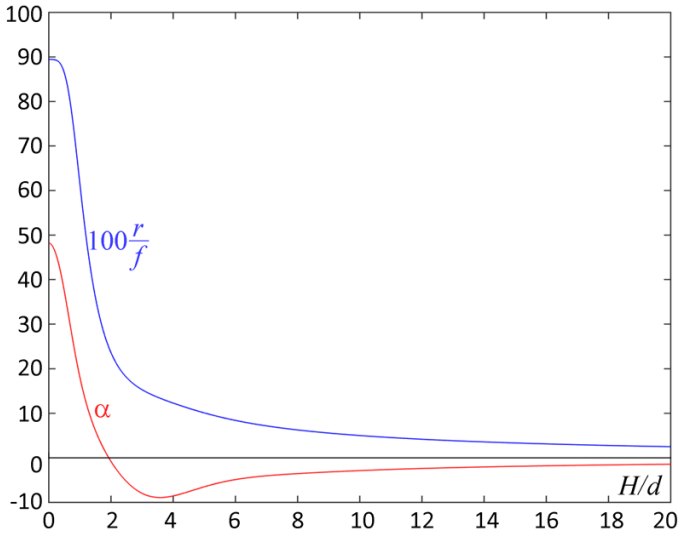

Figure 4: The friction factor r (scaled and magnified) and angle α of veering (in degrees) that are the solutions to Equations (54)-(55).

Now that we have identified an acceptable reduction, we can extract the corresponding expression of the bottom stress. Writing Equations (48)-(49) as

$$-f\bar{v} = -fv_g + \frac{\tau_x}{\rho H} - \frac{\tau_{bx}}{\rho H} \tag{56}$$

$$+f\bar{u} = +fu_g + \frac{\tau_y}{\rho H} - \frac{\tau_{by}}{\rho H} \tag{57}$$

to serve as the definitions of the bottom stress components (τ_{bx}, τ_{by}), we obtain:

$$\tau_{bx} = (1-\cos\alpha)\ \tau_x + \sin\alpha\ \tau_y + \rho r H \bar{u} \tag{58}$$

$$\tau_{by} = (1-\cos\alpha)\ \tau_y - \sin\alpha\ \tau_x + \rho r H \bar{v} \ . \tag{59}$$

Thus, the proper way to parameterize the bottom stress is to add a surface stress component to a classical term proportional to the depth-averaged velocity. The importance of this surface stress component decreases

for increasing depth because the angle α vanishes as $H/d \to \infty$, as Figure 4 shows. The need to include the surface stress in the formulation of the bottom stress was already recognized by Nihoul (1977 - Equation (61)), but without recourse to the preceding developments, he did not make provision for veering and obtained a coefficient (m in his notation) with a weak and monotonic dependence on the water depth.

5 Conclusions

We investigated the case of rotating shallow water when Ekman dynamics extend throughout the water column instead of being restricted to thin boundary layers under surface and above bottom. Although this had been investigated in parts some time ago, the complexity of the algebra obscured some of the flow properties. Chiefly, Welander (1957) did identify that the depth-averaged flow vorticity depends not only on the surface stress curl (as it does in deep water) but also on its divergence; however, he did not document the importance of the new term. Using less complicated algebraic manipulations, we show here that the divergence term vanishes in both limits of very deep ($H/d \to \infty$) and very shallow water ($H/d \to 0$), with largest significance on the order of 20% for a water depth around 3 times the Ekman layer thickness $d = \sqrt{2\nu/f}$.

The physical interpretation of the dependence of the vertical velocity, and hence of the flow vorticity, on both curl and divergence of the surface stress is as follows. In reduced depth, where the top and bottom Ekman layers overlap, each of these layers[†] is, in a sense, incomplete. This implies that the vertically averaged transport in the top layer is at less than the full 90° to the surface stress. The divergence of this transport, which induces the vertical velocity, thus contains two terms: The transport component perpendicular to the surface stress contributes the classical term proportional to the curl, while the component parallel to the surface stress (caused by the departure from 90°) contributes a second term proportional to the divergence of the surface stress. The latter contribution vanishes when the depth becomes sufficient large to create a decoupling of both Ekman layers, with the transport in the top Ekamn layer then oriented at 90° to the surface stress.

Although the surface stress divergence effect cannot be dominant in the presence of a finite surface stress curl, it will dominate wherever and whenever the surface stress curl is weak or nil in water with depth comparable to the Ekman layer thickness. This means that a curl-free but non-uniform wind stress on a shallow sea or lake can, through the dual action of rotation and friction, generate vorticity in the wind-driven currents. To the knowledge of the authors, this had not been identified earlier.

This analysis also has implications for the reduction of three-dimensional hydrodynamics to a two-dimensional model. We show that, for such a reduction to be faithful to 3D dynamics, it is inappropriate to align the bottom stress with the depth-averaged velocity, and this cast doubts on numerous simulations performed over the last five decades with two-dimensional models. We further show that invoking a veering angle between bottom stress and depth-averaged flow still does not cure the problem. Instead, the bottom stress must be taken as consisting of two components, one depending on the surface stress (with veering) and the other depending on the depth-averaged flow (without veering).

ACKNOWLEDGEMENTS

The first author expresses his gratitude to Prof. GertJan van Heijst for having organized the 2017 Symposium on Shallow Flows in Eindhoven. The second author wishes to acknowledge past support from the Belgian Fund for Scientific Research (F.R.S. – FNRS) in recognition of the fact that some elements of the present paper originated while he served as Research Associate of the FNRS earlier in his career.

[†]There is some subjectivity as to where the top layer ends and the bottom one begins, obviously, but this does not need to be resolved for the sake of the argument made here.

REFERENCES

Bennetts, D. A., and L. M. Hocking, 1973: On nonlinear Ekman and Stewartson layers in a rotating fluid. *Proc. R. Soc. Lon. A*, **333**, 469-489.

Cheng, R. T., T. M. Powell, and T. M. Dillon, 1976: Numerical models of wind-driven circulation in lakes. *Appl. Math. Modelling*, **1**, 141-159.

Cushman-Roisin, B., and J.-M. Beckers, 2011: *Introduction to Geophysical Fluid Dynamics – Physical and Numerical Aspects*. Academic Press, 2nd ed., 828 pages.

Ekman, V. W., 1923: Über Horizontalzirkulation bei winderzeugten Meeresströmungen. *Arkiv Mat. Astr. Fysik*, **17**, No. 26.

Forristall, G. Z., 1974: Three-dimensional structure of storm-generated currents. *J. Geophys. Res.*, **79**, No. 18, 2721-2729.

Heaps, N. S., 1969: A two-dimensional numerical sea model. *Philos. Trans. R. Soc. A*, **265**, 93-137.

Jelesnianski, C. P., 1970: Bottom stress time-history in linearized equations of motion for storm surges. *Mon. Weather Rev.*, **9**8, No. 6, 462-478.

Józsa, J., 2014: On the internal boundary layer related wind stress curl and its role in generating shallow lake circulations. *J. Hydrol. Hydromech.*, **62(1)**, 16-23. doi: 10.2478/johh-2014-0004.

Lenz, S., R. T. Guza, S. Elgar, F. Feddersen, T. H. C. Herbers, 1999: Momentum balances on the North Carolina inner shelf. *J. Geophys. Res. Oceans*, **104**, 18,205-18,226.

Lick, W., 1976: Numerical modeling of lake currents. *Ann. Rev. Earth and Planetary Sci.*, **4**, 49-74.

Lynch, D. R., and C. B. Officer, 1985: Analytic test cases for three-dimensional hydrodynamic models. *Int. J. Numer. Methods in Fluids*, **5**, 529-543.

Nihoul, J. C. J., 1977: Three-dimensional model of tides and storm surges in a shallow well-mixed continental sea. *Dyn. Atmos. Oceans*, **2**, 29-47.

Price, J. J., R. A. Weller, and R. R. Schudlich, 1987: Wind-driven ocean currents and Ekman transport. *Science*, **238**, No. 4833, 1534-1538.

Schwab, D. J., 1983: Numerical simulation of low-frequency current fluctuations in Lake Michigan. *J. Phys. Oceanogr.*, **13**, 2213-2224.

Weisberg, R. H., and L. Zhang, 2008: Hurricane storm surge simulations comparing three-dimensional with two-dimensional formulations based on an Ivan-like storm over the Tampa Bay, Florida region. *J. Geophys. Res. Oceans*, **113**, doi:10.1029/2008JC005115.

Welander, P., 1957: Wind action on a shallow sea: Some generalizations of Ekman's theory. *Tellus*, **9**, 45-52.